Chapter 4

Fusion Barrier Distribution: Concept and Experiments

As we saw in the last chapter the solution of the coupled equations in the simplified approach is equivalent to splitting of the single interaction barrier into a spectrum of barriers which are weighted with some factors say W_b $(=|U_{b0}|^2)$ with the condition that $\Sigma_b W_b = 1$. This is the eigen channel approach where each eigen channel is associated with a potential $V(r) + \lambda_b$ which forms a potential barrier of height $B_b = V(R_B) + \lambda_b$ at the interaction distance R_B. This spectrum of barriers in the eigen channel approach is referred to as the "barrier distribution" and is supposed to contain all information about the channels which are coupled. Rowley *et al.*, [1, 2] proposed in 1991 that the distribution of barriers could be extracted directly from precise fusion cross section measurement through a simple and elegant mathematical transformation. Subsequent measurements of fusion barrier distribution have clearly shown characteristic features reflecting the coupling specific to the internal structure of the colliding nuclei demonstrating a new richness in this field.

In this chapter we discuss the theoretical concepts of barrier distribution and its experimental realisation. Attempts to extract barrier distribution from extreme back angle quasi-elastic scattering excitation function are also discussed. These two techniques can be used in a complimentary manner. A review of the experimental barrier distribution for reactions that highlight specific couplings is given. The im-

portance of exact coupled channel calculations in explaining the barrier distributions is also highlighted.

4.1 Representation of the Barrier Distribution

In the case of a rotational nucleus, where the classical picture of a deformed object oriented in different directions in space is appropriate, it is easy to visualise and appreciate the existence of a distribution of fusion barriers. The same is not obvious for a vibrational nuclei, hence one has to see then what is the situation in a general case. Classically, the transmission probability is a step function which goes from one to zero at an energy equal to the height of the barrier. Tunneling effects smear the step function into a smoother function (for a parabolic barrier this smooth function is a Fermi function). Hence the energy derivative of the transmission probability is a narrow peak centered around the barrier energy. If several barriers are present due to channel couplings, the energy derivative of the transmission probability will become a series of peaks corresponding to the energies of the different barriers. The heights of the peaks give the relative weights which the different barriers contribute to the total transmission probability. In the eigen channel approach we can assume that the total fusion cross section is the weighted sum of the transmission through each eigen barrier. If the barrier for each eigen channel is located at the same inter nuclear distance R_B, the transmission coefficient can be recovered from the fusion excitation function provided also that the angular momentum dependence of the transmission coefficient T_ℓ, can be reproduced by a shift in energy *i.e.*

$$T_\ell(E) = T_0(E') \tag{4.1}$$

where $E' = E - \frac{\ell(\ell+1)\hbar^2}{2\mu R_b^2}$

Making this substitution for T_ℓ in the equation,

$$\sigma_{fus}(E) = \frac{\pi}{k^2}\sum_{\ell=0}^{\infty}(2\ell+1)T_\ell \tag{4.2}$$

we can easily arrive at the following form for the transmission coefficient;

$$T_\ell(E) = \frac{1}{\pi R_B^2}\left(\frac{d\ E'\sigma_{fus}(E')}{dE'}\right) \tag{4.3}$$

As said before the transmission function displays a jump each time the energy goes past one of the barriers. This property is exploited to obtain the barrier distribution by further differentiation with respect to energy.

$$\frac{dT(E)}{dE} = \frac{1}{\pi R_B^2}\frac{d^2}{dE^2}[E\sigma_{fus}(E)] \tag{4.4}$$

The transmission coefficient and the corresponding barrier distribution for the $^{16}O + {}^{144}Sm$ case is shown in Fig. 4.1.

Putting in the classical form for fusion cross section in the above formula yields δ-functions at the energies corresponding to the barriers which are weighted with $(\pi R_B^2 \times W_b)$. This is the barrier distribution $D(E, B_b)$. To include tunneling we plug in the Wong's formula for fusion cross section. Double differentiation of $E\sigma_{fus}(E)$ with respect to energy again yields

$$\frac{1}{\pi R_B^2}\frac{d^2}{dE^2}[E\sigma_{fus}(E)] = \left[\frac{2\pi}{\hbar\omega_0}\frac{e^x}{(1+e^x)^2}\right] = G^f(E, B_b) \tag{4.5}$$

where $x = (2\pi/\hbar\omega_0)(E - B_b)$ and $G^f(E, B_b)$ is a function which peaks at each barrier. The function $G^f(E, B_b)$ satisfies $\int G^f(x)dx = 1$ and they become δ function in the limit $\hbar\omega_0 \to 0$. The full width at half maximum of $G^f(E, B_b)$ is

$$\Delta E_{FWHM} = 0.56\ \hbar\omega_0 \approx 2 - 3\ \text{MeV} \tag{4.6}$$

Thus we have an expression for the fusion barrier distribution in a general case.

$$D^f(E) = \frac{1}{\pi R_B^2}\frac{d^2}{dE^2}[E\sigma_{fus}(E)] \tag{4.7}$$

4.1.1 $D^f(E)$ from Experimental Data

In the case of experimental data the derivative cannot be obtained analytically, but they have to be approximated with a point difference formula. For the second

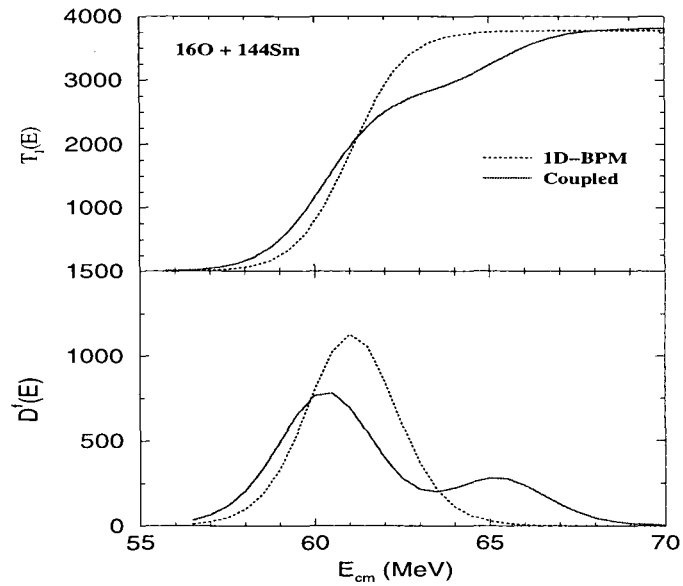

Figure 4.1: The transmission coefficient T_ℓ as a function of energy for the system $^{16}O + ^{144}Sm$ and the corresponding barrier distribution for the uncoupled and coupled case.

derivative with respect to energy of $E\sigma_{fus}(E)$ the point difference formula is given by

$$D^f(E) = \frac{E\sigma_{fus}(E+\Delta E) - 2E\sigma_{fus}(E) + E\sigma_{fus}(E-\Delta E)}{\Delta E^2} \tag{4.8}$$

where ΔE is the energy step used to calculate the second derivative. Obviously a small energy step ΔE approximates the analytic derivative better and increases the sensitivity of the structure. However for a fixed experimental uncertainty δ of the cross section the absolute experimental error in $D^f(E)$ is given by

$$\Delta D^f \approx \delta\sqrt{6}\frac{E\sigma_{fus}}{(\delta E)^2} \tag{4.9}$$

One can see that the errors increase with energy and cross section. So the barrier distribution extracted from experimental cross section is less defined at high energies where cross sections are higher. Also a smaller δE which is required for higher sensitivity increases the error. Thus a compromise has to be found between sensitivity

and precision. Generally in most cases a ΔE of 2 MeV is used as a good choice as the distribution has an inherent width of 2 - 3 MeV due to tunneling.

The formalism presented above is strictly valid in the eigen channel model of fusion which results from the solution of the coupled channels equation in the simplified approach. This approach ignores that the different fusion barriers can have different radii. However both full theoretical calculations and experimental data clearly indicate that evaluating $d^2(E\sigma)/dE^2$ generates a "distribution" with well defined structures, giving significant insight into the role of the target and projectile structure in the fusion process. This form of representation of the experimental data has the advantage of clean identification of the coupling scheme which is not possible by observing the fusion cross section alone.

However the extraction of the second derivative from the experimental cross section is not a trivial job. It amounts to taking small differences between large cross sections. One needs very high quality data to be able to do so. The quality of data is basically decided by two things, one the precision and the other accuracy. By precision of data is meant the reproducibility of the data, and it is basically dependent on random errors. It is these random errors which affect the calculation of the barrier distribution as three neighbouring points are involved in getting one value of the second derivative. The accuracy of the data depends on systematic errors and does not affect the calculation of barrier distribution. Hence one needs to minimise all kinds of random errors to be able to extract a meaningful barrier distribution.

4.2 Barrier Distribution from Scattering Data

The experimental barrier distribution, $D^f(E)$ is a direct consequence of the coupling of the entrance channel to the internal degrees of freedom of the colliding nuclei. The flux transmitted through the barriers amounts to fusion while the reflected flux goes into quasi-elastic reactions like elastic, inelastic scattering and transfer

reactions. Since the total flux is conserved, the coupling interactions that influence fusion should also have effect on the other channels. In fact, the coupled channels formalism describes heavy ion reactions in a unified manner. It is therefore expected that the distribution of potential barriers may be evident in the excitation functions measured for other reaction channels also [3]. The coupled channels does suggest that some information about the distribution of barriers of a reaction might be contained in the backward angle excitation functions for the quasi-elastic reactions.

Classically for the case of a single potential barrier B_k and a head on collision, *i.e* the scattering angle $\theta = 180°$, there is a direct relationship between the differential fusion cross section $d\sigma_{fus}(E)$ and the quasi-elastic scattering differential cross section $d\sigma_{qel}(E)$ based on the simple conservation of flux. The conservation of flux can be represented for $\ell = 0$ partial wave as

$$T(E) + R(E) \equiv 1 \tag{4.10}$$

where T(E) and R(E) are the transmission and reflection coefficient respectively. As we saw in the previous section

$$T(E) = \frac{1}{\pi R_B^2} \frac{d}{dE}[E\sigma_{fus}(E)] \tag{4.11}$$

while the reflection coefficient is equal to the ratio of the differential cross section for the quasi elastic and Rutherford scattering

$$R(E) = \frac{d\sigma_{qel}}{d\sigma_R}(E, \theta = 180°) \tag{4.12}$$

The differential of T(E) with respect to energy gives the barrier distribution $D^f(E, B_b)$ *i.e*

$$\frac{dT}{dE} = \frac{1}{\pi R_B^2} \frac{d^2}{dE^2}[E\sigma_{fus}(E)] = D^f(E, B_b) \tag{4.13}$$

Combining all the above equations it follows

$$D^f(E, B_b) = \frac{dT}{dE} = -\frac{dR}{dE} = -\frac{d}{dE}\left[\frac{d\sigma_{qel}}{d\sigma_R}(E, \theta = 180°)\right] \tag{4.14}$$

Thus classically for a single barrier the barrier distribution $D(E, B_b)$ can be obtained by differentiating $d\sigma_{qel}/d\sigma_R(E)$ at 180° with respect to energy. Quantum mechanically also one can get

$$D^{qel}(E) = -\frac{d}{dE}\left[\frac{d\sigma_{qel}}{d\sigma_R}(E, \theta = 180°)\right] \equiv G^{qel}(E, B_b) \tag{4.15}$$

where $G^{qel}(E, B_b)$ is also a narrowly peaked function at the position of the barrier. Hence it defines an alternative representation of the barrier distribution, which is valid for a single barrier as also for the case of several barriers. The above concepts have been tested by exact coupled channels calculations. The calculated representation $D^f(E)$ and $D^{qel}(E)$ of the barrier distribution are found to be very similar.

4.2.1 $D^{qel}(E)$ from Experimental Data

As said before one needs to measure quasi-elastic scattering excitation function at 180° to be able to extract the barrier distribution. Experimentally, it is difficult to measure scattering excitation functions at a laboratory angle $\theta_{lab} = 180°$, hence experiments are carried out at angles as close to 180° as possible. In order to compare the shape of the barrier distribution obtained from these measurements with that for 180° scattering the energy scale for the former has to be reduced by the centrifugal energy E_{cent}. Assuming Rutherford orbits, the centrifugal energy is given by

$$E_{cent} = E_{cm}\frac{cosec(\theta_{cm}/2) - 1}{cosec(\theta_{cm}/2) + 1} \tag{4.16}$$

where θ_{cm} is the detection angle in the centre of mass system. It has been shown that the shape of $D^{qel}(E)$ changes only slightly for angles close to 180°, however oscillatory behaviour of $D^{qel}(E)$ at below barrier energies is seen for some systems [4] even at laboratory angles very close to 180°. These oscillations are associated with diffraction effects which can be avoided at extreme back angles.

In this thesis we have reported on the measurement of 180° *quasi-elastic scattering excitation function.*

The barrier distribution $D^{qel}(E)$ is extracted from the experimental data using the point difference formula

$$D^{qel}(E) \approx -\frac{d\sigma_{qel}/d\sigma_R(E+0.5\Delta E) - d\sigma_{qel}/d\sigma_R(E-0.5\Delta E)}{\Delta E} \tag{4.17}$$

where ΔE is the step size used. In order to compare $D^{qel}(E)$ with $D^f(E)$, the latter has to be divided by the asymptotic classical fusion cross section πR_B^2. The experimental data show that the two distributions are very similar. The important difference however lies in the way in which the errors in cross section are propagated to the barrier distribution. There are large uncertainties for $D^f(E)$ at higher energies. In contrast, it follows from the point difference formula that for $D^{qel}(E)$, the uncertainties are given by

$$\Delta D^{qel} \approx \frac{\delta\sqrt{2}}{\Delta E}\left(\frac{d\sigma_{qel}}{d\sigma_R}(E)\right) \tag{4.18}$$

which decrease with energy as the quasi-elastic cross section falls rapidly.

Thus the alternative representation of the barrier distribution as given by $D^{qel}(E)$ is better defined at higher energies. Measurements performed by Timmers *et al.*, [4] show that though the $D^{qel}(E)$ shows the general features of $D^f(E)$, its sensitivity is reduced at higher energies ($^{16}O + ^{144}Sm$ system). More recently Rowley *et al.*, [5] showed that the effects of strong coupling are present in the barrier distribution from elastic scattering but are smoothened out since different eigen barriers have phase differences. Also the effects are smoothened by weak coupling, which appear in first order in the elastic scattering cross section, but only in the second order in fusion cross sections. Hence it would be important to treat the phase problem properly in order to obtain information on barrier distribution from elastic scattering data.

4.3 Review of Barrier Distribution Measurements

In the following sections, a review of the important barrier distribution measurements which highlight the advantage gained in displaying the data in this form is given.

4.3.1 Reactions Involving Rotational Nuclei

Since the existence of a distribution of barriers is best justified in the case of rotational nuclei, the first measurements were performed on rotational nuclei. This served basically as a test of the concept. The first measurements were performed at ANU for the systems $^{16}O + ^{154}Sm$, ^{186}W [6]. Here the beam ^{16}O was inert and the targets are known to have static deformation. The most important result of this first measurement was the sensitivity of the barrier distribution not only to the quadrupole deformation but also to the hexadecapole deformation. The dramatic difference in the shapes of the experimental distributions for the two systems was mainly due to the differences in the sign of the β_4. The results also showed that, for statically deformed nuclei, the function $d^2(E\sigma_{fus}(E))/dE^2$ does indeed return a sensible representation of the barrier distribution which is expected from the classical picture.

Other measurements like $^{40}Ca + ^{192}Os,^{194}Pt$ [7] performed at the University of Washington also explored the effects of the nuclear shapes on the barrier structure and excitation function.

4.3.2 Reactions Involving Vibrational Nuclei

Since the existence of the barrier distribution is not obvious for vibrational nuclei it was essential to perform measurements involving vibrational nuclei in order to establish the general formalism.

The $^{16}O + ^{144}Sm$ Reaction

The experimental barrier distribution for the $^{16}O + ^{144}Sm$ system [8] exhibited a distinct two peaked structure, with the main strength around 60 MeV and a peak with smaller strength near 65 MeV. An excellent representation of the excitation function and the double peaked structure of the barrier distribution was obtained by including couplings to the 2^+ and the 3^- states of ^{144}Sm, the latter having the

dominant effect. This established the barrier distribution picture even in the case where the excitation energies are not zero as in the eigen channel approach.

The ^{58}Ni + ^{60}Ni Reaction

The experimental study of ^{58}Ni + ^{60}Ni system [9] revealed for the first time the existence of a barrier distribution with several well defined peaks that could only be explained by multi-phonon coupling. Full calculations including coupling upto four phonon states gave a very good account of the excitation function and also reproduced the three peaked barrier distribution.

The ^{16}O + ^{208}Pb Reaction

The re-measurement of the fission excitation function for ^{16}O + ^{208}Pb was performed at the Australian National University using ^{16}O beams from the 14UD Pelletron accelerator [10]. The purpose of this work was to find the cause of the previous disagreement between theory and data by comparing the new barrier distribution with exact coupled channels calculations and to identify the dominant coupling in the fusion of ^{16}O + ^{208}Pb. Coupling to the single- and 2-phonon states of ^{208}Pb, correctly taking into account the excitation energy and phonon character of these states, particle transfers and the effects of varying the diffuseness of the nuclear potential were all explored. However no satisfactory simultaneous description of the experimental barrier distribution and the fusion excitation function could be obtained. This has put a question mark on our understanding of the fusion process.

4.3.3 Reactions Involving Transfer Coupling

The importance of transfer coupling in enhancing fusion is well established however quantitative verification has not been possible partly because of the sparse transfer data. Moreover transfer coupling in the weak coupling limit are difficult to isolate from other strong coupling cases like coupling to inelastic channels in the excitation function. The barrier distribution can help in unfolding this degeneracy. Most of

the experiments performed to address this problem studied systems with positive Q-value neutron transfer channels because they would give rise to a barrier lower in energy than the inelastic coupling.

The comparison of the measured barrier distribution for the ^{17}O + ^{144}Sm reaction [8] with that for ^{16}O +^{144}Sm showed unambiguously that for the ^{17}O projectile, coupling to the 1n-stripping channels with a positive Q-value produced a barrier lower than in the case of the ^{16}O system. Many other reactions have been studied, like ^{40}Ca + $^{46,48,50}Ti$ [11], $^{32,36}S$ + ^{110}Pd, ^{40}Ca + $^{116,124}Sn$ [12, 13] and barrier distributions have been extracted to investigate the effects of two or more neutron transfer channels with positive Q-values. The ^{40}Ca + $^{90,96}Zr$ [14] system was studied to see the effect of sequential transfer of several neutrons. The experimental barrier distribution for the ^{40}Ca + ^{96}Zr case was flat and rather structure-less extending to low energies. This was in sharp contrast to the distribution for ^{90}Zr which showed well defined peaks. Calculations indicate that sequential neutron transfer, rather than single step neutron transfer in the case of ^{40}Ca + ^{96}Zr is required to explain the data. Thus the effect of single neutron transfer channels is seen as change of slope of the excitation function at the lowest energies whereas for multi-neutron sequential transfer there is significant effect on both the excitation function and barrier distribution at energies below and close to the barrier.

4.3.4 Barrier Distribution from Quasi-Elastic Scattering

Although for many systems quasi-elastic angular distributions have been measured, excitation functions have only rarely been measured with high precision. In order to test the technique for extracting barrier distribution from 180° excitation function, precise measurements were performed for the systems ^{16}O + ^{92}Zr, ^{144}Sm, ^{154}Sm and ^{186}W [4] at the Australian National University. These reactions were selected because the experimental distributions $D^f(E)$ are known so that a comparison of $D^f(E)$ and $D^{qel}(E)$ is possible. The detection angles for the ^{16}O + ^{92}Zr were

$\theta_{lab} = 143°$ and 155°, while for the $^{16}O + ^{144}Sm$ they were $\theta_{lab} = 143°$, 155° and 170°. For the systems $^{16}O + ^{154}Sm$, ^{186}W, the detection angle was $\theta_{lab} = 170°$. For all four systems the quasi-elastic excitation functions $d\sigma_{qel}/d\sigma_R(E)$ show a smooth monotonic decrease with energy which is different for each system. The barrier distribution $D^{qel}(E)$ was extracted using an energy step of 2 MeV. The extracted distributions reflect the barrier distribution of the reaction. They were compared with $D^f(E)$ which were divided by the classical cross section πR_B^2 to facilitate comparision. For the target nuclei ^{154}Sm, ^{186}W and ^{92}Zr the two distributions are consistent with each other. However, $D^{qel}(E)$ is different from $D^f(E)$ for the ^{144}Sm target. The high energy peak in $D^f(E)$ is absent in $D^{qel}(E)$. This suggests that there is a certain loss of sensitivity at high energy in some case as pointed out earlier.

More measurements have been performed like ^{16}O, $^{32}S + ^{208}Pb$, and $^{40}Ca + ^{90,96}Zr$ [15] however none of these have been performed at a laboratory scattering angle of 180°. In most of the measurements a general consistency has been seen in the barrier distribution extracted from fusion excitation function and that obtained from back angle quasi-elastic scattering excitation function suggesting that this can be used to extract complimentary information.

4.4 Review of Coupled Channels Calculations

The very first coupled channels calculations for heavy-ion fusion were performed under several approximation so as to simplify the calculations. These calculations used the adiabatic approximation, neglecting the finite excitation energies of the surface vibrations. However, excitation energies of the order of 1 MeV as typically encountered in vibrational nuclei are too large to be ignored. Also these calculations assumed a linear coupling to the quadrupole or octupole surface vibrations and quadrupole deformations. This is clearly insufficient for coupling to a rotational band. In the case of vibrational coupling, only single phonon states were included in the calculations. Within these limitations, the simplified calculations were successful

in explaining the sub-barrier enhancement in many cases. However, the power of new precise data and its visualisation through the experimental barrier distribution technique exposed the limitations of these calculations. The quality of the existing data now makes it possible to quantitatively explore the effect of the approximations introduced in the theoretical calculations. In the following sections we will see the effect of non-linear couplings, the effect of the anharmonicities in the vibrational spectra and the effect of coupling to high lying states on the fusion process and the refinement in the calculations which can take care of them.

4.4.1 Effect of Non-Linear Couplings

An important component in the theoretical description of the sub-barrier fusion data is the effect of non-linear couplings. Though the linear coupling approximation reproduces the experimental data for very asymmetric systems, it does not explain the data for heavier and nearly symmetric systems [16, 17]. The effect of higher order couplings on the barrier distributions in the limit of zero excitation energy has been discussed by Balantekin *et al.* [18] in the framework of the interacting boson model (IBM). Esbensen and Landowne [19] showed the importance of second order coupling terms. The quadratic coupling approximation was shown to describe well the fusion cross sections and angular momentum distributions for the ^{58,64}Ni + ^{92,100}Mo reactions [20]. Later Stefanini [9] performed coupled channels calculations including coupling to all orders and finite excitation energy of nuclear vibration for the system ^{58}Ni + ^{60}Ni.

Hagino *et al.* [21] showed the importance of high order coupling in the analysis of symmetric as well as very asymmetric systems also. They found that for the ^{64}Ni + ^{92,96}Zr reactions, terms beyond those in the quadratic coupling approximation result in further enhancement of the fusion cross section at sub-barrier energies. The inclusion of the coupling to all orders is crucial to reproduce the experimental fusion cross sections and average angular momenta. For the asymmetric systems

^{16}O + ^{112}Cd, ^{144}Sm also, the higher order coupling resulted in a non negligible enhancement of the fusion cross section and a significant modification of the barrier distribution and the average angular momenta.

4.4.2 Effect of Anharmonicities of Nuclear Vibrations

The analysis of ^{58}Ni + ^{60}Ni [9] and ^{36}S + ^{110}Pd [12] data showed that while one-phonon space clearly fails in describing the barrier distribution for these systems, the agreement with data improved successively as one included more phonons in the calculations. These calculations were performed in the harmonic oscillator approximation. However for the case of ^{16}O + ^{144}Sm [6] it was found that inclusion of the double phonon excitations of ^{144}Sm in the calculations in the harmonic limit destroys the agreement between the experimental fusion barrier distribution and calculations. Hagino *et al.* [22] demonstrated that the anharmonic properties of the quadrupole and octupole vibrational excitations in ^{144}Sm strongly influence the shape of the barrier distribution and their inclusion leads to good agreement between the data and theoretical predictions. In fact, these studies show that the fusion barrier distribution does not depend so much on the excitation energies of the multi-phonon states once the single phonon quadrupole and octupole states are fixed. The main effect comes from the re-orientation effects as well as the deviation of the transition probability from the harmonic limit.

4.4.3 Effect of High Lying States

It was found that for the system, ^{16}O + ^{144}Sm, the good theoretical representation of the experimental fusion barrier distribution obtained by neglecting the couplings to projectile states was destroyed when the 3^- state of ^{16}O is included. In contrast to this, the ^{40}Ca + ^{192}Os, ^{194}Pt reactions [7] which also involved a closed shell projectile, showed a characteristic structure with a high energy peak which could be explained by including coupling to the octupole state of ^{40}Ca. Hagino *et al.* [23] pointed

out that the observed discrepancy is due to the inadequacy of the linear coupling approximation used in the calculation. Their calculations including coupling to ^{16}O states to all orders reproduces the shape of the experimental distribution apart from a energy shift. The calculations by Hagino *et al.* for the $^{40}Ca + ^{192}Os, ^{194}Pt$ reactions which treat the coupling to the 3^- states of ^{40}Ca to all orders produce a higher energy peak in quantitative agreement with the experimental observation.

The calculations with full order coupling thus show that while the dominant effect of the excitation of the ^{16}O octupole state at 6.1 MeV is simply to renormalise the static potential, the coupling to the 3^- state in ^{40}Ca at 3.7 MeV introduces well defined peaks in the barrier distribution for the systems $^{40}Ca + ^{192}Os, ^{194}Pt$. However for reactions of ^{40}Ca with light targets where coupling effects are weak, coupling to the states of ^{40}Ca just renormalises the potential. These calculations therefore suggest a natural limit to the energy of states which need to be considered explicitly in the coupled channel calculations.

Bibliography

[1] N. Rowley, G. R.Satchler, and P. H. Stelson, Phys. Lett. **B254**, 25 (1991).

[2] N. Rowley, Nucl. Phys. **A538**, 205c (1992).

[3] A. .T. Kruppa, P. Romain, M. A.Nagarajan, N. Rowley, Nucl. Phys. . **A560**, 845 (1993).

[4] H. Timmers, J. R. Leigh, M. Dasgupta, D. J. Hinde, R. C. Lemmon, J. C. Mein, C. R. Morton, J. O. Newton, N. Rowley, Nucl. Phys. **A584**, 190 (1994).

[5] N. Rowley, H. Timmers, J. R. Leigh, M. Dasgupta, D. J. Hinde, J. C. Mein, C. R. Morton, J. O. Newton, Phys. Lett. **B373**, 23 (1996).

[6] J. R. Leigh, M. Dasgupta, D. J. Hinde, J. C. Mein, C. R. Morton, R. C. Lemmon, J. P. Lestone, J. O. Newton, H. Timmers, J. X. Wei, and N. Rowley, Phys. Rev. **C52**, 3151 (1995).

[7] J. D. Bierman, P. Chan, J. F. Liang, M. P. Kelly, A. A. Sonzogni, and R. Vandenbosch, Phys. Rev. Lett. **76**, 1587 (1996).

[8] C. R. Morton, M. Dasgupta, D. J. Hinde, J. R. Leigh, R.C . Lemmone, J. P. Lestone, J. C. Mein, J. O. Newton, H. Timmers, N. Rowley, and A. T. Kruppa, Phys. Rev. Lett. **72**, 4074 (1994).

[9] A. M. Stefanini, D. Ackermann, L. Corradi, D. R. Napoli, C. Petrache, P. Spolaore, P. Bednarczyk, H. Q. Zhang, S. Beghini, G. Montagnoli, L. Mueller,

F. Scarlassara, G. F. Segato, F. Sorame, and N. Rowley, Phys. Rev. Lett. **74**, 864 (1995).

[10] C. R. Morton, A. C. Berriman, M. Dasgupta, D. J. Hinde, J. O. Newton, K. Hagino, I. J. Thompson, Phys. Rev. **C60**, 044608 (1999).

[11] A. A. Sonzogni, J. D. Bierman, M. P. Kelly, J. P. Lestone, J. F. Liang, R. Vandenbosch, Phys. Rev. **C57**, 722 (1998).

[12] A. M. Stefanini, D. Ackermann, L. Corradi, J. H. He, S. Beghini, G. Montagnoli, F. Scarlassara, G. F. Segato, Phys. Rev. **C52**, R1727 (1995).

[13] A. M. Stefanini, L. Corradi, D. Ackermann, C. J. Lin, L. F. Zheng, S. Beghini, G. Montagnoli, F. Scarlassara, G. F. Segato, Nuovo Cemento **111A**, 895 (1998).

[14] H. Timmers, L. Corradi, A. M. Stefanini, D. Ackermann J. H. He, S. Beghini, G. Montagnoli, F. Scarlassara, G. F. Segato, N. Rowley, Phys. Lett. **B399**, 35 (1997).

[15] H. Timmers, D. Ackermann, S. Beghini, L. Corradi, J. H. He, G. Montagnoli, F. Scarlassara, A. M. Stefanini, N. Rowley, Nucl. Phys. **A633**, 421 (1998).

[16] R. Vandenbosch, Annu. Rev. Nucl. Sci. **42**, 447 (1992), and references therein

[17] A. Charlop, J. Bierman, Z. Drebi, A. Garcia, S. Gil, D. Prindle, A. Sonzogni, R. Vandenbosch, and D. Ye, Phys. Rev. **C51**, 628 (1995).

[18] A. B. Balentakin, J. R. Bennett, S. Kuyucak, Phys. Rev. **C48**, 1269 (1993); 1079 (1994).

[19] H. Esbensen and S. Landowne, Phys. Rev. **C35**, 2090 (1987).

[20] K. E. Rehm, H. Esbensen, J. Gehring, B. Glagola, D. Henderson, W. Kutschera, M. Paul, F. Soramel, A. H. Wuosmma, Phys. Lett. **B317**, 31 (1993).

[21] K. Hagino, N. Takigawa, M. Dasgupta, D. J. Hinde, J. R. Leigh, Phys. Rev. **C55**, 276 (1997).

[22] K. Hagino, N. Takigawa, S. Kuyucak, Phys. Rev. Lett. **79**, 2943 (1997).

[23] K. Hagino, N. Takigawa, M. Dasgupta, D. J. Hinde, J. R. Leigh, Phys. Rev. Lett. **79**, 2014 (1997).